Slow-Binding Inhibition of γ-Glutamyl Transpeptidase by γ-boroGlu

Ross L. Stein,*,‡ Carl DeCicco,§ David Nelson,§ and Beth Thomas‡

Departments of Chemical Enzymology and Medicinal Chemistry, DuPont Pharmaceuticals Company, Wilmington, Delaware 19880

Received January 23, 2001; Revised Manuscript Received March 19, 2001

ABSTRACT: γ-Glutamyl transpeptidase (γGTase) catalyzes the transfer of the γ-glutamyl moiety of γ-glutamyl-derived peptides, such as glutathione (γGlu-Cys-Gly), and anilides, such as γ-glutamyl-7-amido-4-methylcoumarin (γGlu-AMC), to acceptor molecules, including water and various dipeptides. These acyl-transfer reactions all occur through a common acyl−enzyme intermediate formed from attack of an active site hydroxyl on the γ-carbonyl carbon of γGlu-X with displacement of X. In this paper, we report that γGTase is potently inhibited by the γ-boronic acid analogue of L-glutamic acid, 3-amino-3-carboxypropaneboronic acid (γ-boroGlu). We propose that γ-boroGlu adds to the active site hydroxyl of γGTase to form a covalent, tetrahedral adduct that resembles tetrahedral transition states and intermediates that occur along the reaction pathway for γGTase-catalyzed reactions. Our studies demonstrate that γ-boroGlu is a competitive inhibitor of the γGTase-catalyzed hydrolysis of γGlu-AMC with a K_i value of 35 nM. Kinetics of inhibition studies allow us to estimate the following values: $k_{on} = 400\ mM^{-1}\ s^{-1}$ and $k_{off} = 0.02\ s^{-1}$. We also found that γ-boroGlu is an uncompetitive inhibitor of Gly-Gly-promoted transamidation of γGlu-AMC. This observation is consistent with the kinetic mechanism we determined for γGTase-catalyzed transamidation of γGlu-AMC by Gly-Gly to form γGlu-Gly-Gly. To probe rate-limiting transition states for γGTase catalysis and inhibition, we determined solvent deuterium isotope effects. Solvent isotope effects on k_c/K_m for hydrolysis of γGlu-AMC and k_{on} for inhibition by γ-boroGlu are identical and equal unity, suggesting that the processes governed by these rate constants are both rate-limited by a step that is insensitive to solvent deuterium such as a conformational fluctuation of the initially formed E−S or E−I complex. In contrast, the solvent isotope effect on k_c is 2.4. k_c is rate-limited by hydrolysis of the acyl−enzyme intermediate that is formed during reaction of γGTase with γGlu-AMC. Thus, the magnitude of this isotope effect suggests the formation of a catalytically important protonic bridge in the rate-limiting transition state for deacylation.

γ-Glutamyl transpeptidase is a heterodimeric glycoprotein composed of 45 and 22 kDa subunits (*1*−*3*). It is expressed on the luminal surface of glands and ducts and is at its highest concentration on renal proximal tubules where it plays an important role in glutathione metabolism, including a role in drug excretion via the mercapturic acid pathway (*2*, *3*). γGTase[1] catalyzes the transfer of a γ-glutamyl moiety from glutathione and related compounds to water and other nucleophiles, such as certain amino acids and dipeptides (*2*, *4*).

γGTase catalyzes three acyl-transfer reactions of γ-glutamyl amides: hydrolysis, autotransamidation, and transamidation (*4*). These reactions are thought to proceed through a common acyl−enzyme intermediate as illustrated in the mechanism of Scheme 1. According to this mechanism, the acyl−enzyme intermediate can partition one of three ways. In the absence of added nucleophiles and at a low substrate concentration, the acyl−enzyme intermediate reacts predominantly with water to produce the simple product of hydrolysis, glutamic acid. At higher substrate concentrations, the acyl−enzyme substrate combines with a second molecule of γGlu-X to form the E-O-γGlu:γGlu-X binary complex. Autotransamidation occurs within this binary complex through the attack of the α-amine of γGlu-X on the acyl−enzyme intermediate to form the (γGlu-X)−γGlu complex. Finally, in the presence of certain nucleophilic species that are recognized by γGTase (e.g., Gly-Gly and other dipeptides), the nucleophile can compete for the acyl−enzyme intermediate to form the E-O-γGlu:Nuc complex, from

Scheme 1: Mechanism of γ-Glutamyl Transpeptidase

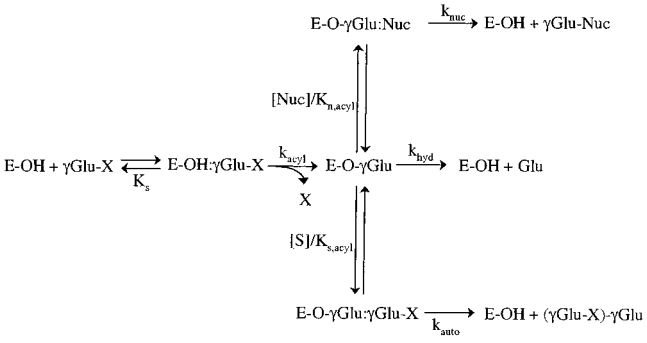

* To whom correspondence should be addressed: DuPont Pharmaceuticals Co., Experimental Station, E400/4462, Route 141 and Henry Clay Road, Wilmington, DE 19880. Phone: (302) 695-1605. Fax: (302) 695-8313. E-mail: Ross.L.Stein@dupontpharma.com.

‡ Department of Chemical Enzymology.

§ Department of Medicinal Chemistry.

[1] Abbreviations: γGTase, γ-glutamyl transpeptidase; γGlu-AMC, γ-glutamyl-7-amido-4-methylcoumarin; γ-boroGlu, 3-amino-3-carboxypropaneboronic acid.

10.1021/bi010147i CCC: $20.00
Published on Web 04/17/2001

which transamidation occurs to produce γGlu-Nuc. The rate law for the overall mechanism is given in eq 1.

$$\frac{v_{ss}}{[\gamma\text{GTase}]} = \frac{\left(\frac{k_{acyl}k_{deacyl}}{k_{acyl}+k_{deacyl}}\right)[\gamma\text{Glu-X}]}{K_s\left(\frac{k_{deacyl}}{k_{acyl}+k_{deacyl}}\right)+[\gamma\text{Glu-X}]} \quad (1)$$

where

$$k_{deacyl} = k_{hyd} + \frac{k_{auto}[\gamma\text{Glu-X}]}{K_{s,acyl}+[\gamma\text{Glu-X}]} + \frac{k_{nuc}[\text{Nuc}]}{K_{n,acyl}+[\text{Nuc}]} \quad (2)$$

Simplification of eq 2, and thus eq 1, will of course occur in situations of no nucleophile and low substrate concentration.

As illustrated in Scheme 1, reactions of γGTase are thought to proceed according to a mechanism involving a catalytic hydroxyl group. It is currently unclear if this hydroxyl is contributed from a serine residue or a threonine residue. On the one hand, recent mutagenesis experiments (*5*) have confirmed early chemical modification studies (*6*, *7*) that suggest the catalytic involvement of an active site serine. The mutagenesis studies may have, in fact, revealed a unique mechanism involving the possible participation of two adjacent serine residues, Ser^{451} and Ser^{452}. When either residue is individually mutated to alanine, activity is reduced to ~1% of the wild-type enzyme. The double mutant S451A/S452A has essentially no activity (i.e., 0.002% of the wild-type activity). It is currently unclear how these residues would participate in catalysis.

However, at odds with these studies is a recent paper reporting the efficient and competitive inactivation of γGTase by the mechanism-based inhibitor 2-amino-4-(fluorophosphono)butanoic acid (k_{inact}/K_i = 50 mM^{-1} s^{-1}) with specific phosphonylation of the N-terminal Thr^{391} of the catalytic subunit (*20*). These and other results reported in this paper suggest that Thr^{391} is the catalytic nucleophile of γGTase and that γGTase is a member of the family of N-terminal nucleophile hydrolases.

Regardless of the amino acid residue that is involved, Ser^{451}/Ser^{454} or Thr^{391}, it does seem clear that an active site hydroxyl is involved as the catalytic nucleophile. Part of the evidence supporting this comes from studies in which it was found that the complex formed from covalent interaction of serine with boric acid (see Scheme 2) is a 50 μM inhibitor of the hydrolytic action of γGTase, while uncomplexed serine is only a 12 mM inhibitor (*7*). In the studies reported herein, we extended these earlier observations by examining the inhibition of γGTase by the γ-boronate analogue of glutamic acid, γ-boroGlu[2] (see Scheme 2). Our studies demonstrate that γ-boroGlu is a potent, time-dependent inhibitor of γGTase and probe features of the inhibition mechanism.

[2] During the preparation of the manuscript, a paper appeared [London, R. E., and Gabel, S. A. (2001) *Arch. Biochem. Biophys. 385*, 250−258] reporting the inhibition of γGTase and glutamic pyruvic transaminase by γ-boroGlu. While this paper reported that the inhibitor was competive with the substrate γ-glutamyl-*p*-nitroanilide for γGTase, no other aspects of the mechanism were probed, such as the time dependence of inhibition, dipeptide-promoted transpeptidation, or protonic bridging in the transition state for inhibitor binding.

Scheme 2: Interaction of γGlutamyl Transpeptidase with Substrates and Inhibitors

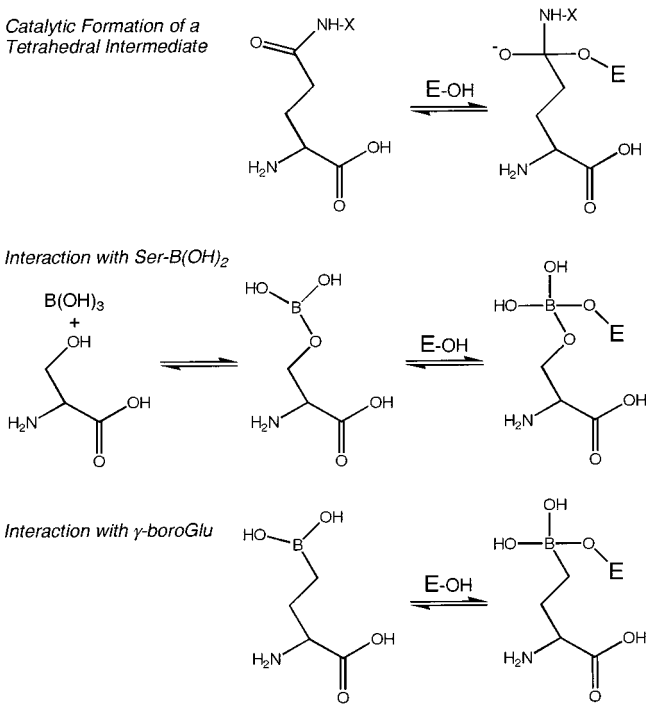

MATERIALS AND METHODS

General. Buffer salts, γ-Glu-AMC, Gly-Gly, and γ-glutamyl transpeptidase (G4756, porcine kidney, lyophilized powder) were from Sigma Chemical Co. γ-BoroGlu was synthesized as described in the literature (*19*) with some modifications (unpublished studies of C. DeCicco and D. Nelson). The assay buffer was 0.1 M Tris-HCl (pH 8.1) (*4*, *5*). A 2.2 mg/mL (~19 μM) stock solution of γGTase was prepared in assay buffer and stored in 100 μL aliquots at −20 °C. A 1.0 mM stock solution of γGlu-AMC was prepared in a 50/50 methanol/assay buffer mixture and stored at −20 °C.

Kinetic Methods. In a typical kinetic run, a 1−100 μL aliquot of stock γGlu-AMC was added to 2.00 mL of assay buffer in a 3 mL cuvette, and the cuvette was placed in the jacketed cell holder of a Hitachi fluorometer. The reaction temperature was maintained at 37.0 ± 0.1 °C by a circulating water bath. After the reaction solution had reached thermal equilibrium (~5 min), γGTase was added to the cuvette to initiate the reaction. Reaction progress was monitored by the increase in fluorescence (λ_{ex} = 380 nm, λ_{em} = 438) that accompanies hydrolysis of γGlu-AMC to liberate AMC. For each kinetic run, 100−3000 data points, corresponding to {time, fluorescence intensity} pairs, were collected with a personal computer interfaced with the fluorometer.

RESULTS

Steady-State Kinetics of Catalysis by γ-Glutamyl Transpeptidase

Hydrolysis and Autotransamidation. The dependence of the steady-state velocity on the concentration of γGlu-AMC is shown in Figure 1A and clearly indicates departure from simple Michaelis−Menten kinetics. These data suggest some mechanism of substrate activation in which a second molecule of substrate binds to the Michaelis complex to

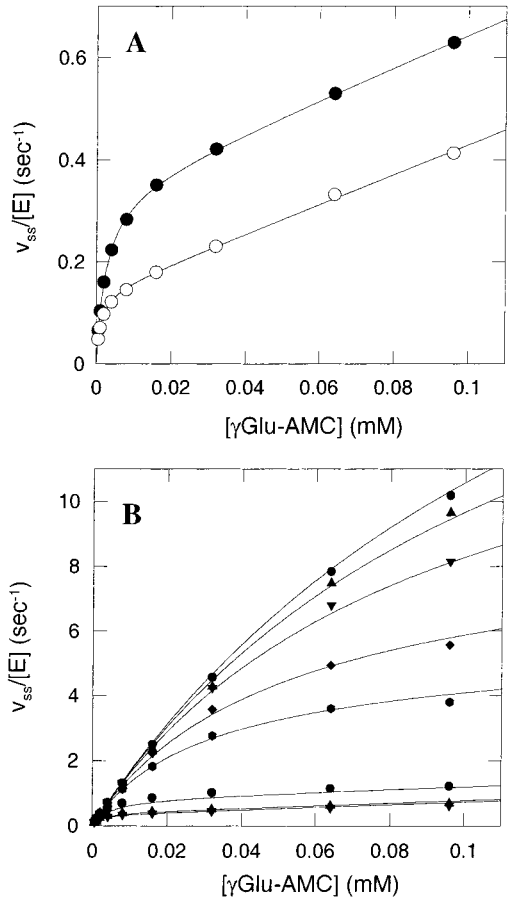

FIGURE 1: Dependence of steady-state velocity on substrate concentration for γGTase catalysis. (A) Steady-state velocities for the γGTase-catalyzed hydrolysis and autotransamidation of γGlu-AMC were determined at nine substrate concentrations (0.5 μM ≤ [γGlu-AMC]$_o$ ≤ 96 μM) in H_2O and D_2O [pH 8.1 and the equivalent pD (● and ○, respectively)]. Solid lines describing the dependence of v_{ss}/[E]$_o$ on [S]$_o$ were drawn according to eq 3 with the apparent steady-state kinetic parameters of Table 2. (B) Steady-state velocities for the γGTase-catalyzed hydrolysis, autotransamidation, and Gly-Gly-promoted transamidation of γGlu-AMC were determined as a function of γGlu-AMC concentration at eight fixed Gly-Gly concentrations (0, 0.01, 0.1, 1, 2, 5, 10, and 20 mM). Solid lines represent a global fit of the data set according to eq 1 with k_{deacyl} defined by eq 7 and k_{hyd} constrained to 0.36 s^{-1}. The best-fit values are summarized in Table 1. Reaction conditions were as follows: 0.1 M Tris-HCl at pH 8.1 and 37 °C, [γGTase] = 10 (A) or 2 nM (B).

produce a ternary complex that turns over more efficiently than the simple Michaelis complex. This general mechanism is described by the rate expression of eq 3

$$\frac{v_{ss}}{[E]} = \frac{(k_c + k_{act}'[S])[S]}{K_m + [S]} \quad (3)$$

in which k_c and K_m have their usual meaning and k_{act}' is the second-order rate constant for reaction of the substrate with the Michaelis complex to form product. The data in Figure 1A (●) can be fit to this expression to provide the best-fit values: $k_c = 0.35 \pm 0.01$ s^{-1}, $K_m = 2.5 \pm 0.1$ μM, and $k_{act}' = 3.1 \pm 0.1$ mM^{-1} s^{-1}.

Substrate activation for γGTase has ample precedent in the literature (*4*, *5*) and is explained in the context of Scheme 1 and eqs 1 and 2 under the condition of no added nucleophile. As the concentration of γGlu-AMC increases, γGlu-AMC binds to the acyl−enzyme intermediate to form a species within which autotransamidation occurs. The linearity of the dependence of steady-state velocity on γGlu-AMC concentrations between 20 and 90 μM indicates that these concentrations are much lower than $K_{s,acyl}$ of Scheme 1 and that the E-O-γGlu:γGlu-AMC species does not accumulate in the steady state. Thus, eq 1 can be simplified to

$$\frac{v_{ss}}{[E]} = \frac{\left[\frac{k_{acyl}(k_{hyd} + k_{auto}'[S])}{k_{acyl} + k_{hyd} + k_{auto}'[S]}\right][S]}{K_s\left(\frac{k_{hyd} + k_{auto}'[S]}{k_{acyl} + k_{hyd} + k_{auto}'[S]}\right) + [S]} \quad (4)$$

in which $k_{auto}' = k_{auto}/K_{s,acyl}$. Note that eqs 1 and 4 are related by the expressions

$$k_c = \frac{k_{acyl}(k_{hyd} + k_{auto}'[S])}{k_{acyl} + k_{hyd} + k_{auto}'[S]} \quad (5)$$

$$K_m = K_s\left(\frac{k_{hyd} + k_{auto}'[S]}{k_{acyl} + k_{hyd} + k_{auto}'[S]}\right) \quad (6)$$

Attempts at fitting the data in Figure 1A to eq 4 failed because of nonconvergence and revealed that there is no single set of parameter values that best describe the data. In particular, we found that k_{acyl} and K_s are coupled; that is, these two parameters vary together to maintain a constant ratio, k_{acyl}/K_s, of 141 mM^{-1} s^{-1}. However, the fitting routine did converge when k_{acyl} and K_s were constrained to values greater than 3 s^{-1} and 21 μM, respectively, while maintaining a $k_{acyl}/K_{s,acyl}$ of 141 mM^{-1} s^{-1}. Under these conditions, we calculated the following values: $k_{hyd} = 0.36 \pm 0.01$ s^{-1} and $k_{auto}' = 3.8 \pm 0.4$ mM^{-1} s^{-1}.

Hydrolysis, Autotransamidation, and Transamidation. Figure 1B shows the dependence of steady-state velocity on the concentration of γGlu-AMC at eight fixed concentrations of the Gly-Gly nucleophile ranging from 0 to 20 mM. These data can be described by eq 1 with

$$k_{deacyl} = k_{hyd} + k_{auto}'[\gamma\text{Glu-X}] + \frac{k_{nuc}[Nuc]}{K_{n,acyl} + [Nuc]} \quad (7)$$

where γGlu-X is γGlu-AMC and Nuc is Gly-Gly. Best-fit parameters for a global fit of the data set could be determined by constraining k_{hyd} to the value determined above of 0.36 s^{-1}. To explore how sensitive the fitting results are to the value assigned to k_{hyd}, k_{hyd} values ranging from 0.1 to 0.5 s^{-1} were also used. The results of this fitting exercise are summarized in Table 1. As judged by both the errors associated with the calculated parameters and the X^2 values, it is clear that the best fit to the data of Figure 1B is obtained when k_{hyd} is constrained to 0.36 s^{-1}. It is these values that are used to draw the solid lines in Figure 1B.

Analysis of Progress Curves for the Slow-Binding Inhibition of γ-Glutamyl Transpeptidase by γ-BoroGlu

In experiments in which γGTase is added to a solution of γGlu-AMC and γ-boroGlu, the rate of production of AMC decreases with time until a final, steady-state velocity is

Table 1: Analysis of Steady-State Kinetic Parameter Estimation for Catalysis by γ-Glutamyl Transpeptidase[a]

k_{hyd} (s^{-1})	k_{auto}' (mM^{-1} s^{-1})	k_{acyl} (s^{-1})	K_s (mM)	k_{nuc} (s^{-1})	$K_{n,acyl}$ (mM)	10^4X^2
0.10	7.1 ± 0.7	280 ± 180	1.6 ± 0.9	37 ± 4	6.9 ± 0.7	160
0.20	5.7 ± 0.6	300 ± 160	1.7 ± 0.9	37 ± 3	6.9 ± 0.6	119
0.30	4.3 ± 0.5	133 ± 60	0.8 ± 0.3	45 ± 6	8.3 ± 1.2	93
0.36	3.5 ± 0.5	190 ± 83	1.1 ± 0.4	40 ± 3	7.5 ± 0.7	83
0.40	2.9 ± 0.5	220 ± 92	1.3 ± 0.5	40 ± 3	7.4 ± 0.7	72
0.50	1.6 ± 0.5	270 ± 360	1.5 ± 2.1	39 ± 6	7.2 ± 1.2	72

[a] The data of Figure 1 were fit to eq 1 with k_{deacyl} defined as in eq 7 and k_{hyd} constrained to the indicated values. The overall quality of the fit was assessed on the basis of (i) errors associated with the calculated parameters, (ii) values of X^2, where $X^2 = \sum\text{residuals}^2/(N - n - 1)$, where N is the number of data points and n is the number of parameters, and (iii) visual inspection of the data with the theoretical lines drawn.

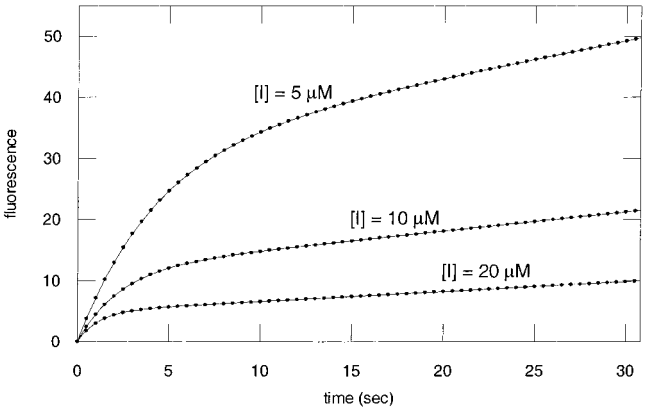

FIGURE 2: Reaction progress curves for the inhibition of γGTase by γ-boroGlu. Enzyme was added to a thermally equilibrated solution of γGlu-AMC and γ-boroGlu and the release of AMC product monitored as a function of time. Solid lines were drawn using eq 8 and the following best-fit parameters. When [γ-boroGlu] = 5 μM, v_o = 7.98 FI/s, v_{ss} = 0.600 FI/s, and k_{obs} = 0.236 s^{-1}. When [γ-boroGlu] = 10 μM, v_o = 5.43 FI/s, v_{ss} = 0.314 FI/s, and k_{obs} = 0.433 s^{-1}. When [γ-boroGlu] = 20 μM, v_o = 4.38 FI/s, v_{ss} = 0.164 FI/s, and k_{obs} = 0.854 s^{-1}. Reaction conditions were as follows: 0.1 M Tris-HCl at pH 8.1 and 37 °C, [γGTase] = 20 nM, [γGlu-AMC] = 20 μM.

reached. Examples of typical progress curves are shown in Figure 2 and are diagnostic of slow-binding inhibition. These progress curves were fit to eq 8, the standard equation for slow-binding inhibition (*8*, *9*)

$$[P] = v_s t + \left(\frac{v_o - v_s}{k_{obs}}\right)(1 - e^{-k_{obs}t}) \quad (8)$$

to allow estimation of the initial velocity v_o, the final steady-state velocity v_{ss}, and the pseudo-first-order rate constant k_{obs} for the approach to steady state.

Dependence of Inhibition on the Concentration of γ-BoroGlu

Inhibition progress curves were recorded at various concentrations of γ-boroGlu at a single concentration of γGlu-AMC (20 μM) and analyzed according to eq 8. The dependencies of v_{ss} and k_{obs} on [γ-boroGlu] are shown in panels A and B of Figure 3, respectively.

The dependence of v_{ss} on [γ-boroGlu] can be described by a simple binding isotherm with a $K_{i,app}$ of 0.31 μM and indicates complete inhibition of γGTase by γ-boroGlu and a 1:1 stoichiometry for binding of the inhibitor to the enzyme with no necessity for higher-order inhibitor terms in the rate equation. If we assume competitive inhibition (see below), we calculate a K_i value of 34 nM ([S] = 20 μM; K_m = 2.5 μM).

The dependence of k_{obs} on [γ-boroGlu] is linear and suggests a simple inhibition mechanism in which the enzyme combines with the inhibitor to form the E−I complex with the accumulation of no intermediates (*8*, *9*). Thus, the dependence of k_{obs} on inhibitor concentration obeys the relationship

$$k_{obs} = k_{on,app}[I] + k_{off} \quad (9)$$

where $k_{on,app}$ is the apparent, mechanism-dependent second-order rate constant for formation of the E−I complex and k_{off} is the first-order rate constant for the decomposition of this complex back to the free enzyme and inhibitor. The slope of the line of Figure 3B is $k_{on,app}$ and is equal to 41 mM^{-1} s^{-1}. The *y*-intercept of this line is −0.0015 ± 0.022 s^{-1} and, thus, indicates that k_{off} is less than ∼0.02 s^{-1} and cannot be defined by this experiment. For competitive inhibition, $k_{on,app} = k_{on}/(1 + [S]/K_m)$, and assuming this mechanism (see below), we can calculate a k_{on} value of 370 mM^{-1} s^{-1}.

Dependence of Inhibition on the Concentration of γGlu-AMC

Inhibition progress curves were recorded at various concentrations of γGlu-AMC at a single concentration γ-boroGlu (1 μM) and analyzed according to eq 8. The dependencies of $K_{i,app}$ and k_{obs} on [γGlu-AMC] are shown in panels A and B of Figure 4, respectively.

At each substrate concentration, we used the measured steady-state velocities to calculate the term $[I]/[(v_c/v_i) - 1]$, where v_c is the control velocity in the absence of inhibitor and v_i is the steady-state velocity in the presence of inhibitor. This term is equal to $K_{i,app}$ at each of the substrate concentrations that were examined. As shown in Figure 4A, $K_{i,app}$ increases with increasing substrate concentration, suggestive of competitive inhibition. However, the dependence of $K_{i,app}$ on [γGlu-AMC] is not linear, as expected for competitive inhibition of a simple enzymatic reaction, but rather is curved. To describe these data, we must use the rate law of eq 10 which takes into account the full mechanism of Scheme 1

$$K_{i,app} = \frac{[I]}{\frac{v_c}{v_i} - 1} = \frac{[I]}{\frac{k_c[S]/(K_m + [S])}{k_c[S]/[K_m(1 + [I]/K_i) + [S]]}} \quad (10)$$

with no added nucleophile. k_c and K_m are defined by eqs 5 and 6, respectively.

To find the best-fit value for K_i, we constrained the parameters of eq 10 to the values given in Table 1 for the case where k_{hyd} = 0.36 s^{-1}. When the data were treated in this way, we determined a K_i of 33 ± 1 nM. This value of K_i agrees with the value of 34 nM determined above and gives us confidence in claiming that γ-boroGlu is a competitive inhibitor of the γGTase-catalyzed hydrolysis of γGlu-AMC.

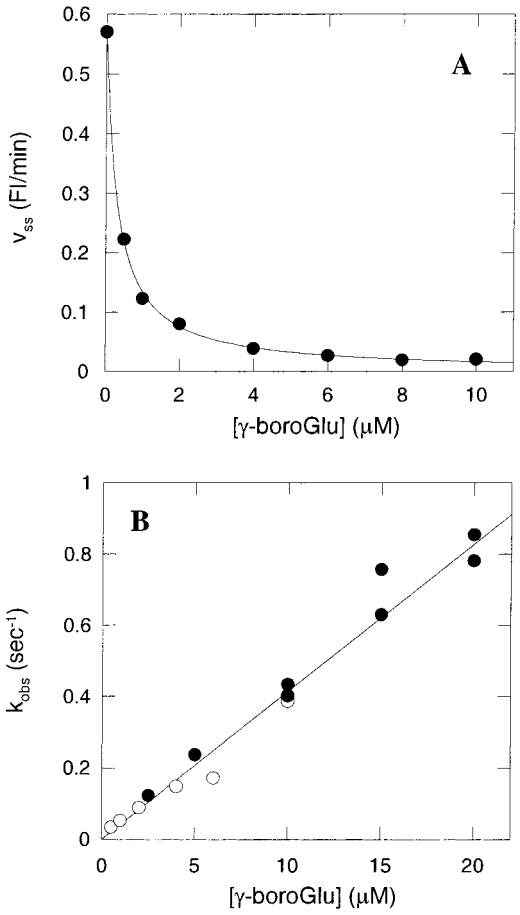

FIGURE 3: Dependence of the inhibition of γGTase on γ-boroGlu concentration. Reaction progress curves for the inhibition of γGTase by γ-boroGlu were determined at various inhibitor concentrations and analyzed according to eq 8. (A) Steady-state velocities from this analysis were plotted as a function of γ-boroGlu concentration. The solid line was drawn using a simple binding isotherm [i.e., $v_{ss} = v_{ss,max}/(1 + [I]/K_{i,app})$] and the following best-fit parameters: $v_{ss,max} = 0.571 \pm 0.007$ FI/min and $K_{i,app} = 0.305 \pm 0.016$ μM. (B) Values of k_{obs} from this analysis were plotted as a function of γ-boroGlu concentration. The solid line was drawn using eq 9 and the following best-fit parameters: $k_{on,app} = 41.4 \pm 1.2$ mM^{-1} s^{-1} and $k_{off} = -0.0015 \pm 0.022$ s^{-1}. Reaction conditions were as follows: 0.1 M Tris-HCl at pH 8.1 and 37 °C, [γGlu-AMC] = 20 μM, [γGTase] = 10 nM (panel A and ○ in panel B) or 200 nM (● in panel B).

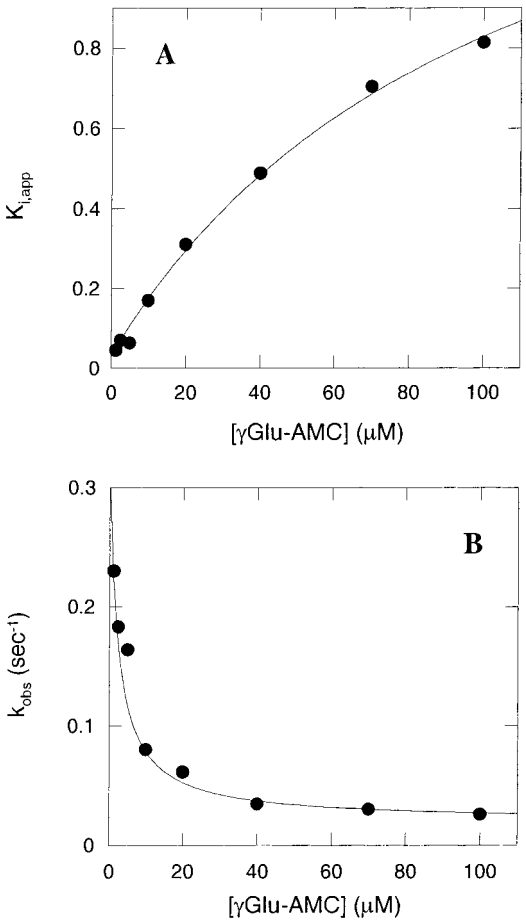

FIGURE 4: Dependence of the inhibition of γGTase by γ-boroGlu on γGlu-AMC concentration. Reaction progress curves for the inhibition of γGTase by γ-boroGlu were determined at various concentrations of γGlu-AMC and analyzed according to eq 8. (A) Values of $K_{i,app}$ (see the text and eq 10 for definition) were plotted as a function of γGlu-AMC concentration. The solid line was drawn using eq 10, with k_c and K_m defined as in eqs 5 and 6, respectively, and parameters from Table 1 ($k_{hyd} = 0.36$ s^{-1}). The best-fit value for K_i is 32.6 ± 0.5 nM. (B) Values of k_{obs} were plotted as a function of γGlu-AMC concentration. The solid line was drawn using eq 11, with K_m defined as in eq 6, and parameters from Table 1 ($k_{hyd} = 0.36$ s^{-1}). Best-fit values are as follows: $k_{on} = (4.0 \pm 0.3) \times 10^5$ M^{-1} s^{-1} and $k_{off} = 0.012 \pm 0.006$ s^{-1}. Reaction conditions were as follows: 0.1 M Tris-HCl at pH 8.1 and 37 °C, [γ-boroGlu] = 1.0 μM, [γGTase] = 10 nM.

The dependence of k_{obs} on [γGlu-AMC] is shown in Figure 4B and indicates competitive inhibition. For competitive inhibition, the expression of eq 9 is recast as eq 11

$$k_{obs} = \frac{k_{on}}{1 + \frac{[S]}{K_m}}[I] + k_{off} \qquad (11)$$

where K_m is defined by eq 6. To find the best-fit value for k_{on} and k_{off}, we constrained the parameters of eq 11 to the values given in Table 1 for the case where $k_{hyd} = 0.36$ s^{-1}. When the data of Figure 4B are fit in this way, the following best-fit parameters are calculated: $k_{on} = (4.0 \pm 0.3) \times 10^5$ M^{-1} s^{-1} and $k_{off} = 0.012 \pm 0.006$ s^{-1}. The k_{off}/k_{on} ratio equals 30 nM and agrees with our independently determined values of K_i (see above).

Determination of k_{off} for the Inhibition of γ-Glutamyl Transpeptidase by γ-BoroGlu

To determine a more accurate value of k_{off} for the inhibition γ-GTase by γ-boroGlu, we conducted an experiment in which we incubated 15 μM enzyme with 20 μM inhibitor (assay buffer, 10 min) and, at the end of the incubation period, diluted the mixture 1000-fold into assay buffer containing 20 μM γGlu-AMC and recorded the progress curve for production of AMC. Note that at time zero, the reaction solution contains 5 nM free inhibitor, 15 nM enzyme−inhibitor complex, no free enzyme, and 20 μM substrate. Thus, the reaction progress curve reflects the generation of active enzyme from the E−I complex. A typical progress curve is shown in Figure 5 and was fit to eq 8 with the following results: $v_o = 0.003 \pm 0.007$ FI/s, $v_{ss} = 0.285 \pm 0.008$ FI/s, and $k_{obs} = 0.0219 \pm 0.0007$ s^{-1}. The final, steady-state velocity determined in this and replicate experiments is equal to the velocity of control

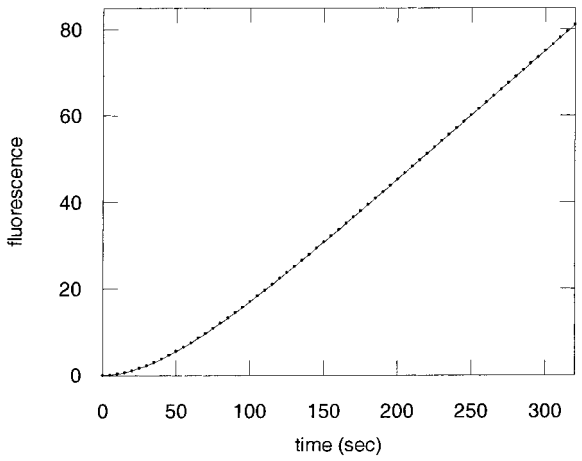

FIGURE 5: Determination of k_{off} for the inhibition of γGTase by γ-boroGlu. Enzyme (15 μM) and inhibitor (20 μM) were incubated for 10 min in assay buffer (0.1 M Tris-HCl at pH 8.1) and then diluted 1000-fold into assay buffer containing 20 μM γGlu-AMC. The reaction progress curve for production of AMC was then recorded and is shown here. The solid line was drawn using eq 8 and the best-fit parameters: $v_o = 0.003 \pm 0.007$ FI/s, $v_{ss} = 0.285 \pm 0.008$ FI/s, and $k_{obs} = 0.0219 \pm 0.0007$ s^{-1}.

reactions where [γGTase] = 15 nM and [γGlu-AMC] = 20 μM. From replicate experiments we calculate a k_{off} of 0.021 ± 0.003 s^{-1}.

Uncompetitive Inhibition by γ-BoroGlu of Gly-Gly-Promoted Transamidation

The mechanism of Scheme 1 predicts that γ-boroGlu will be an uncompetitive inhibitor of Gly-Gly-promoted transamidation of γGlu-AMC. To test this, we determined progress curves as a function of Gly-Gly concentration with constant concentrations of γGlu-AMC and γ-boroGlu (10 and 0.5 μM, respectively). The results of these experiments are shown in Figure 6 as a plot of v_c/v_i versus [Gly-Gly] and agree with theory for an uncompetitive inhibitor in the mechanism of Scheme 1; that is, v_c/v_i should increase hyperbolically with increasing concentrations of added nucleophile. The line through the data was drawn using the expressions of eqs 7 and 12, the parameters of Table 1 ($k_{hyd} = 0.36$ s^{-1}), and a K_i of 26 nM

$$\frac{v_c}{v_i} = \frac{K_s\left(1 + \frac{[I]}{K_i}\right)\left(\frac{k_{deacyl}}{k_{acyl} + k_{deacyl}}\right) + [\gamma\text{Glu-AMC}]}{K_s\left(\frac{k_{deacyl}}{k_{acyl} + k_{deacyl}}\right) + [\gamma\text{Glu-AMC}]} \quad (12)$$

The excellent fit of the line to the data supports not only uncompetitive inhibition by γ-boroGlu of Gly-Gly-promoted transamidation but also the veracity of the mechanism depicted in Scheme 1.

Solvent Isotope Effects on γ-Glutamyl Transpeptidase Catalysis and Inhibition

To explore features of rate-limiting transition states for γGTase catalysis and inhibition, we determined solvent deuterium isotope effects. Figure 1A summarizes data from an experiment in which we measured steady-state reaction velocities as a function of [γGlu-AMC] in light and heavy water at pH 8.1 and an equivalent pD. Best-fit values

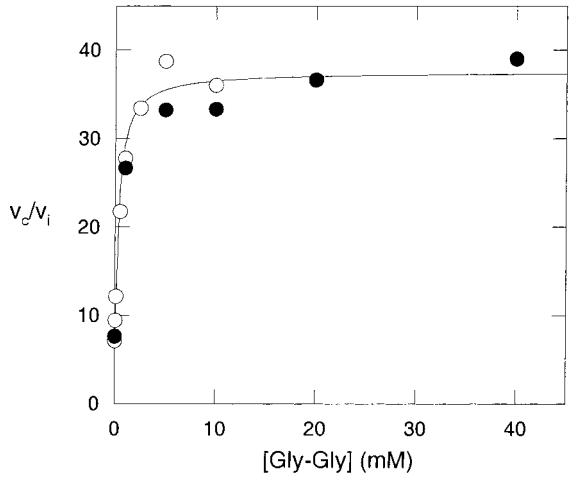

FIGURE 6: Uncompetitive inhibition by γ-boroGlu of the Gly-Gly-promoted transamidation of γGlu-AMC. Reaction progress curves for the inhibition of γGTase by γ-boroGlu were recorded at various concentrations of Gly-Gly and analyzed according to eq 8. These data were used to calculate the v_c/v_i ratios which are plotted here as a function of Gly-Gly concentration. The white and black circles represent two independent experiments. The solid line was drawn using eq 12, with k_{deacyl} defined as in eq 7, parameters from Table 1 ($k_{hyd} = 0.36$ s^{-1}), and a K_i value of 26 nM. Reaction conditions were as follows: 0.1 M Tris-HCl at pH 8.1 and 37 °C, [γGlu-AMC] = 10 μM, [γ-boroGlu] = 1.0 μM, [γGTase] = 2 nM.

Table 2: Solvent Deuterium Isotope Effects for γ-Glutamyl Transpeptidase Catalysis and Inhibition[a]

parameter	H_2O	D_2O	H_2O/D_2O[b]
catalysis			
k_c (s^{-1})	0.353 ± 0.005	0.145 ± 0.004	2.4
K_m (μM)	2.51 ± 0.08	1.09 ± 0.07	2.3
k_c/K_m (mM^{-1} s^{-1})	141 ± 3	133 ± 7	1.1
k_{act}' (mM^{-1} s^{-1})	3.06 ± 0.07	2.89 ± 0.06	1.1
inhibition			
k_{on} (mM^{-1} s^{-1})	447 ± 12	392 ± 18	1.1

[a] Reaction conditions were as follows: 0.1 M Tris-HCl at pH 8.1 and 37 °C. See the text for experimental details. [b] We estimate the errors associated with these isotope effects to be ≤10%.

according to eq 3 together with the solvent isotope effects (i.e., ratios of rate constants in H_2O and D_2O) are summarized in Table 2.

To determine the solvent isotope effect on k_{on}, we recorded inhibition progress curves as described above in H_2O and D_2O and fit them to eq 8 to obtain values of $k_{on,obs}$. Values of $k_{on,obs}$ were multiplied by the term $(1 + [S]/K_{m,L_2O})/[I]$ (L is H or D) to provide the following: $k_{on,H_2O} = 447 \pm 12$ mM^{-1} s^{-1} and $k_{on,D_2O} = 392 \pm 18$ mM^{-1} s^{-1} ($n = 3$). The ratio of these rate constants provides the solvent isotope effect ($^{D_2O}k_{on} = 1.14 \pm 0.06$). These results are summarized in Table 2.

DISCUSSION

Catalysis by γ-Glutamyl Transpeptidase. To provide a mechanistic framework for studies of the inhibition of γGTase by γ-boroGlu, we conducted a detailed analysis of the steady-state kinetics for γGTase catalysis. The results of these experiments agree well with the literature (*1*−*4*) and can be interpreted in the context of the mechanism of Scheme 1. Analysis of these results according to this mechanism allows us to assign the rate constants that are summarized in Scheme 3.

Scheme 3: Mechanism of Inhibition of γ-Glutamyl Transpeptidase by γ-BoroGlu

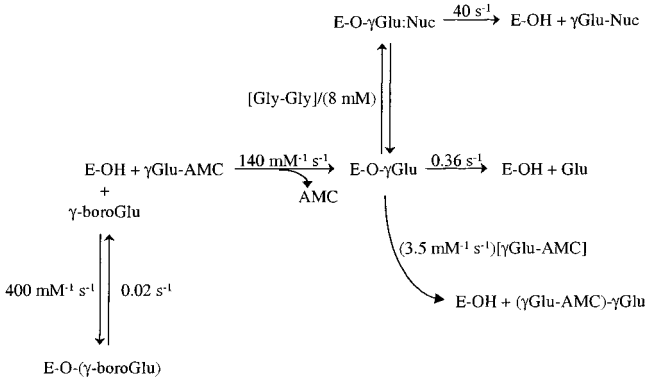

The central feature of the mechanism of catalysis by γGTase is the acyl−enzyme intermediate and how it partitions in response to increasing concentrations of substrate or other nucleophilic species. Our results indicate that this partitioning is insensitive to the structure of dipeptidic nucleophilic species. We found that γGlu-AMC, Gly-Gly, Ala-Gly, and Ser-Gly are all equally effective as nucleophiles toward the acyl−enzyme intermediate; that is, all of these species have similar second-order rate constants for reaction with the acyl−enzyme intermediate of $\sim$4 mM^{-1} s^{-1} (Ala-Gly and Ser-Gly, unpublished results of B. Thomas).

Our kinetic analysis also indicates that the first-order rate constant for acylation of γGTase by γGlu-AMC from within the Michaelis complex is at least 10-fold larger than the rate constant for hydrolysis of the acyl−enzyme intermediate. Rapid acylation and slow, rate-limiting deacylation is not an artifact associated with γGlu-AMC but also occurs during hydrolysis of glutathione and γGlu-*p*-nitroanilide (*10*). These observations fly in the face of our chemical intuition for acyl-transfer reactions, which tells us that attack of an alcohol nucleophile (e.g., active site Ser or Thr) on the carbonyl carbon of an amide to form an ester (e.g., acyl−enzyme intermediate) should be much slower than subsequent hydrolysis of that ester. However, these observations for γGTase do find precedent in the serine protease literature (*11*, *12*, and references within). In all of these cases, including the present, the free energy available from interactions between enzyme and nonreacting portions of the substrate is utilized to stabilize the transition state for acylation, thus allowing this step to proceed faster than the chemically more facile deacylation.

Finally, in our analysis of the steady-state kinetics of γGTase catalysis, we found that the solvent isotope effect on k_c for the hydrolysis of γGlu-AMC is 2.4. Since, as noted above, k_c is identical to k_{hyd}, the magnitude of this isotope effect suggests that the hydrolysis of the acyl−enzyme intermediate is rate-limited by a chemical step that is subject to protolytic catalysis. In contrast, the solvent isotope on k_c/K_m ($=k_{acyl}/K_s$) is 1.1 and suggests that the process governed by this rate constant is rate-limited by some physical step that is not sensitive to solvent deuterium. Likely candidates for this step are conformational fluctuations of the enzyme and release of the first product.

Inhibition of γ-Glutamyl Transpeptidase by γ-BoroGlu. Boronic acids are a well-characterized class of inhibitors of both Ser hydrolases and N-terminal Thr hydrolases. Considering first serine hydrolases, possibly the earliest report comes from Antonov and co-workers (*13*), who in 1970 described a series of alkylboronic acid inhibitors of chymotrypsin. Other simple alkyl- and arylboronic acids were found to be inhibitors of acetylcholinesterase and subtilisin (*14*, *15*). None of these inhibitors was found to be particularly potent or selective, however. For serine proteases, these attributes were not realized until the syntheses of peptide boronic acids that were strongly structurally analogous to efficiently hydrolyzed peptide substrates (*17*). Turning now to N-terminal Thr hydrolases, the literature reports potent inhibition of the proteasome by tripeptide boronic acids (*21*). The most specific examples of these have sub-nanomolar K_i values.

Only weakly potent boronates have thus far been reported for γGTase. These compounds include simple alkylboronic acids (*16*), *m*-formylphenylboronate (*16*), and the serine−boric acid complex (*7*).

In contrast to these latter compounds, γ-boroGlu is a potent inhibitor of γGTase. Our steady-state analysis indicates that it is competitive with γGlu-AMC with a K_i of 35 $\pm$ 5 nM. Our observation that the inhibition is time-dependent allowed us to determine the kinetics of inhibition of γGTase by γ-boroGlu. In these experiments, we first sought to find evidence for the existence of an encounter complex that might form prior to the final, stable complex that accumulates in the steady state. To probe for such an intermediate, we determined the dependence of k_{obs} on inhibitor concentration and found a linear dependence to concentrations as high as 20 μM (Figure 3B). Thus, if such an encounter complex exists, its dissociation constant must be greater than $\sim$100 μM. Given the relative instability of this complex, we can only determine values of k_{on} and k_{off} which are equal to 400 mM^{-1} s^{-1} and 0.02 s^{-1}, respectively.

To probe the rate-limiting transition state for the interaction of γGTase with γ-boroGlu, we determined the solvent deuterium isotope effect on k_{on}. This value is equal to unity and suggests that the process governed by k_{on} is rate-limited by some reaction step that is insensitive to solvent deuterium, such as a conformational change of an initially formed E−I complex. Recall that we also observed a solvent isotope effect of unity for k_c/K_m. Together with their similar magnitudes of 140 and 400 mM^{-1} s^{-1} for k_{on} and k_c/K_m, respectively, the identical solvent isotope effects suggest similar rate-limiting transition states for these two processes.

Finally, while it is tempting to speculate that γ-boroGlu might be a transition-state analogue for γGTase, we lack the data to make this claim. To support such a claim, we would need to find a linear, free energy correlation with a slope near unity between k_c/K_m and K_i for a series of structurally related substrates and boronic acid inhibitors (*18*). However, we may reasonably conclude from our studies that in the final complex that accumulates in the steady state during the inhibition of γGTase by γ-boroGlu, stabilizing interactions are established that do not exist in either the Michaelis complex of γGTase with γGlu-AMC ($K_s \sim 1$ mM, Table 1) or the encounter complex of γGTase with γ-boroGlu ($K_i' \geq 0.1$ mM). Such stabilization is consistent with formation of the addition adduct depicted in Scheme 2 which is structurally analogous to transition states that exist along the reaction pathway for γGTase catalysis.

REFERENCES

1. Meister, A., and Andeson, M. E. (1983) *Annu. Rev. Biochem. 52*, 711−760.
2. Hanigan, M. H. (1998) *Chem.-Biol. Interact. 111*, 333−342.
3. Tate, S. S. (1980) Enzymes of Mercapturic Acid Formation, *Enzymic Basis of Detoxication*, Vol. II, pp 95−120, Acedemic Press, New York.
4. Thompson, G. A., and Meister, A. (1977) *J. Biol. Chem. 252*, 6792−6798.
5. Ikeda, Y., Fujii, J., Anderson, M. E., Taniguchi, N., and Meister, A. (1995) *J. Biol. Chem. 270*, 22223−22228.
6. Inoue, M., Moriuchi, S., and Morino, Y. (1978) *Biochem. Biophys. Res. Commun. 82*, 1183−1188.
7. Tate, S. S., and Meister, A. (1978) *Proc. Natl. Acad. Sci. U.S.A. 75*, 4806−4809.
8. Morrison, J. F. (1982) *Trends Biochem. Sci. 7*, 102−104.
9. Szedlacsek, S., and Duggleby, R. G. (1995) *Methods Enzymol. 249*, 144−180.
10. Tate, S., and Meister, A. (1974) *J. Biol. Chem. 249*, 7593−7602.
11. Rahfeld, J., Schutkowski, M., Faust, J., Neubert, K., Barth, A., and Heins, J. (1991) *Biol. Chem. Hoppe-Seyler 372*, 313−318.
12. Stein, R. L., Viscarello, B. R., and Wildonger, R. A. (1984) *J. Am. Chem. Soc. 106*, 796−798.
13. Antonov, V. K., Ivanina, T. V., Berezin, I. V., and Martinek, K. (1970) *FEBS Lett. 7*, 23−25.
14. Lienhard, G. E., and Koehler, K. A. (1971) *Biochemistry 10*, 2477−2483.
15. Palumaa, P., and Jarv, J. (1984) *Biochim. Biophys. Acta 784*, 35−39.
16. Suenaga, H., Nakashima, K., Mikami, M., Yamamoto, H., James, T. D., Sandanayake, K. R. A. S., and Shinkai, S. (1996) *Recl. Trav. Chim. Pays-Bas 115*, 44−48.
17. Kettner, C. A., and Shenvi, A. B. (1984) *J. Biol. Chem. 259*, 15106−15114.
18. Stein, R. L., Strimpler, A. M., Edwards, P. D., Lewis, J. J., Mauger, R. C., Schwartz, J. A., Stein, M. M., Trainor, D. A., Wildonger, R. A., and Zottola, M. A. (1987) *Biochemistry 26*, 2682−2689.
19. Denniel, V., Bauchat, P., Danion, D., and Danion-Bougot, R. (1996) *Tetrahedron Lett. 37*, 5111−5114.
20. Inoue, M., Hiratake, J., Suzuki, H., Kumagai, H., and Sakaa, L. (2000) *Biochemistry 39*, 7764−7771.
21. Adams, J., Behnke, M., Chen, S., Cruickshank, A., Dick, A., Grenier, L., Klunder, J., Ma, Y.-T., Plamdon, L., and Stein, R. L. (1998) *Bioorg. Med. Chem. Lett. 8*, 333−338.

BI010147I